

## Chapter

# The Electrical Properties of Soils with Their Applications to Agriculture, Geophysics, and Engineering

*Walter G. Fano*

## Abstract

The electric properties of the soils are very important for several sciences like telecommunications, electrical engineering, geophysics, and agriculture. There are semiempirical dielectric models for soils, which represent the real and imaginary part of the dielectric permittivity as the function of the frequency. The measurement methods to obtain the dielectric properties of soils are described for different bands of frequencies from some kHz to several GHz. The parallel plate capacitors are widely used to measure dielectric properties. The transmission line method of a coaxial transmission line can be used in frequency domain and time domain. The time domain technique with transmission lines is usually called time-domain reflectometry (TDR), because it is based on the voltage measurement as a function of time of pulses. The frequency domain technique with transmission lines is based on the reflection coefficient measurement of the transmission line. The transmission line method is described with short load and open-circuit load because it is useful in obtaining the characteristic impedance and the electric permittivity of the media inside.

**Keywords:** soil, dielectric properties, permittivity, models, measurement method

## 1. Introduction

The knowledge of electrical properties of soils in physics and electrical engineering are important for many applications. The long-distance electromagnetic telegraph systems from 1820 are used, with two or more wires to carry the signal and the return currents. It was discovered that the earth could be used as a return path to complete the circuit, making the return wire unnecessary [1]. However, during dry weather, the earth connection often developed a high resistance, requiring water on the earth electrode to enable the telegraph to ring [1].

An important radio propagation and engineering problem has been solved in 1909 by A. Sommerfeld. He has solved the general problem of the effect of the finite conductivity of the ground on the radiation from a short vertical antenna at the surface of a plane earth. The surface wave propagation is produced over real ground for the medium frequency AM radio service, where the attenuation of the electric

field depends on the dielectric properties of the soil, mainly of the dielectric losses [2]. Considering the word “Soil” means the uppermost layer of the earth’s crust, it contains the organic as well as mineral matter. From 1936 up to 1941, Norton, Van der Pol, and Bremmer made the computation of the field strengths at distant points on the flat and spherical Earth’s surface [3, 4].

In agriculture applications, the electrical resistivity methods have been introduced by Conrad Schlumberger in France and Frank Wenner in the United States, for the evaluation of ground electrical resistivity. In saline soils, the electric conductivity measured is high, and the effects of salinity are manifested in the loss of stand, reduced rates of plant growth, reduced yields, and in severe cases, total crop failure [5].

The applications like the protection of electrical generating plant are necessary to provide earth connections with low electrical resistance. The radio transmitting and receiving stations for broadcasting is generally covered by radiation transmitted directly along the ground [6]. In electrical engineering, “ground” is the reference point in an electrical circuit from which voltages are measured.

For archeology, geophysics, engineering, and military applications, the so-called ground-penetrating radar (GPR) is a technique widely used. The radar signal is an electromagnetic wave that propagates through the earth, and its signal is reflected when an object appears or there is a change in the properties of the earth. In order to determine the depth of an object under the ground, it is necessary to know the electrical properties of the soil [7].

## **2. Fundamental concepts**

The equations that relate the electric field (E) and magnetic field (H) are based on the electromagnetic theory formulated by James Clerk Maxwell in 1864, whose validity has allowed great advances in diverse areas, such as telecommunications, electricity, electronics, and materials [8].

Regarding the behavior of the materials under the action of an electric field, in the conductive materials, the charges can move freely, meaning that the electrons are not associated with an atomic nucleus. In the case of dielectric materials, the charges are associated with an atom or specific molecule [9]. There are two main mechanisms where the electric field distorts the distribution of charge in a dielectric, stretching and rotation. The relationship between the electric dipole moment induced under the action of an applied electric field is called atomic electric polarizability  $\vec{p}$  and can be written as

$$\vec{p} = \alpha \vec{E} \quad (1)$$

In a material with an applied electric field, a convenient definition is to consider the contributions of the dipole moment per unit volume; this parameter is called polarization, which is a macroscopic definition instead of a molecular or atomic definition [9, 10]:

$$\vec{P} = \frac{\Delta \vec{p}}{\Delta v} \quad (2)$$

It is evident that the contributions of the electric dipole moment in a volume element  $\Delta v$  are given by the sum of the microscopic contributions  $\vec{p}_m$ ; therefore you can write:

$$\Delta \vec{p} = \sum_m \vec{p}_m \quad (3)$$

And the polarization

$$\vec{P} = \frac{\sum_m \vec{p}_m}{\Delta v} \quad (4)$$

In **Figure 1**, the external electric field applied to a dielectric material and the resulting polarization can be observed.

From the macroscopic point of view in most of the dielectric material, when the electric field is canceled, the polarization in the material will be nullified. In addition, the polarization of the material will vary as the electric field varies, i.e.,

$\vec{P}(E) = \chi(E)\vec{E}$ . The variable  $\chi(E)$  is called electrical susceptibility of the material, and when the electric field applied to the dielectric is not high powered, the relationship between the polarization and the electric field will be linear, as is the case of a soil [10]:

$$\vec{P} = \chi \vec{E} \quad (5)$$

It is convenient to define the electric displacement, because it allows to relate by means of the Gaussian law with the free charges; therefore

$$\vec{D} = \epsilon_0 E + \vec{P} \quad (6)$$

Then

$$\vec{D} = \epsilon_0 E + \chi \vec{E} \quad (7)$$

The electrical permittivity is defined as the relationship between the electric displacement vector  $\vec{D}$  and the electric field vector  $\vec{E}$ , and thus

$$\vec{D} = \epsilon \vec{E} \quad (8)$$

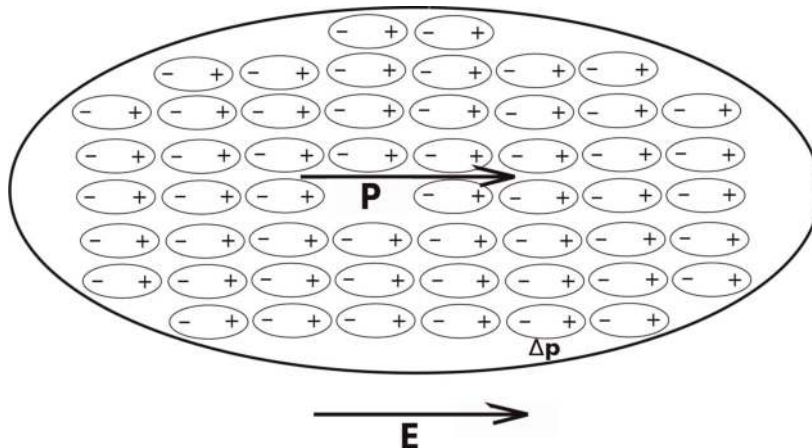


**Figure 1.** Polarization applying external electric field  $E$ , to a dielectric material.

Result

$$\epsilon = \epsilon_0 + \chi \quad (9)$$

It is convenient to define [11]:

$$\chi = \epsilon_0 \chi_r \quad (10)$$

Result

$$\epsilon = \epsilon_0(1 + \chi_r) \quad (11)$$

The electric properties of the material are completely defined by means of  $\epsilon$  or  $\chi$  [10].

In problems with electromagnetic fields, four vectors are defined: E and B; D and H. These vectors are assumed to be finite throughout the entire field, and at all ordinary points to be continuous functions of position and time, with continuous derivatives [12]. The constitutive relations link the vectors of the fields  $\vec{B}$  with  $\vec{H}$  and  $\vec{D}$  with  $\vec{E}$ , usually dependent on the frequency [8]:

$$\begin{aligned} \vec{B} &= \mu(\omega)\vec{H} \\ \vec{D} &= \epsilon(\omega)\vec{E} \\ \vec{J} &= \sigma(\omega)\vec{E} \end{aligned} \quad (12)$$

For the electromagnetic propagation in soils, the parameters  $\mu$ ,  $\epsilon$ , and  $\sigma$  must be determined. The soils are usually nonmagnetic media; therefore the magnetic permeability will be that of the vacuum  $\mu = \mu_0$ , and the variables to be determined will be the electric permittivity  $\epsilon$  and the electric conductivity  $\sigma$ .

The electrical resistivity obtained by soil mapping exhibits a large range of values from  $1\Omega/m$  for saline soil to several  $10^5\Omega/m$  for dry soil overlaying crystalline rocks [13]. In **Figure 2**, the resistivity of different soils can be observed. The electrical conductivity is related to the particle size by the electrical charge density

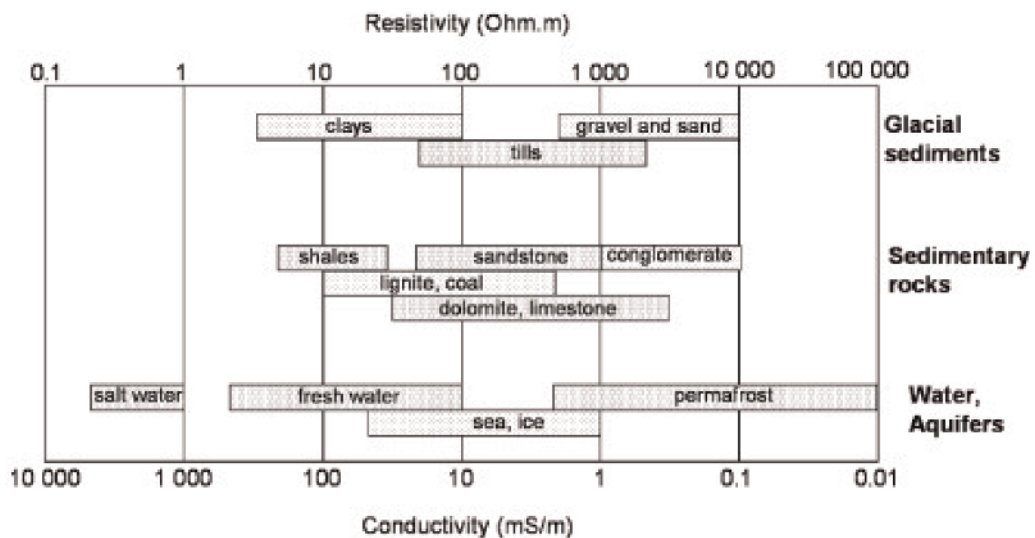


**Figure 2.** Table of electric resistivity [ $\Omega/m$ ] and electric conductivity [ $\sigma/m$ ] of soils (Ref. Samoulian et al.) [13].

at the surface of the solid constituents, like in clay soil; the electrical charges located at the surface of the clay particles lead to greater electrical conductivity than in coarse-textured soils [13].

There are evidences that for compacted soils of clay, it exhibits an anisotropic behavior in the resistivity measured in the horizontal and vertical directions [14].

The literature contains the measurement of the dielectric properties of soils at different frequencies with slotted lines and time-domain reflectometry (TDR) methods [15].

The measured variations of the electric permittivity of soils with fractions of sand, silt, and clay and with volumetric moisture content have been studied for frequency of 440 MHz used by the radar observations [16].

The coaxial probe technique terminated in the material under test has been used to measure the dielectric properties of the vegetation. The dielectric data reported are based on measurements of the amplitude and phase of the reflection coefficient of a coaxial probe [17, 18].

### 3. Transmission line fundamentals

The transmission line method has been used to measure the dielectric properties [19, 20]. These transmission lines are coaxial, quasi-coaxial, and two-wire transmission lines. Consider a transmission line with a homogenous dielectric material inside, and the propagation is transverse electromagnetic mode (TEM), where the electric and magnetic field are perpendicular to the propagation direction; this can be observed in **Figures 3** and **4**.

The separation between the conductive cylinders that form the coax transmission line should be much lower than the wavelength of the signal that propagates, so the transmission line will not be affected by the propagation modes of high orders, such as the  $TE_{11}$  [19].

Coaxial transmission lines are widely used for the transmission of radio-frequency signals and its application in radiocommunications and for broadcasting [21]. The transmission lines allow the connection between a generator or emitter and a load or antenna. The air coaxial transmission line consists of two cylindrical conductors, with air between both conductors. These metallic conductors are those that impose the boarder conditions that must comply with the electric and magnetic fields of the electromagnetic wave that travel inside the line. The coaxial

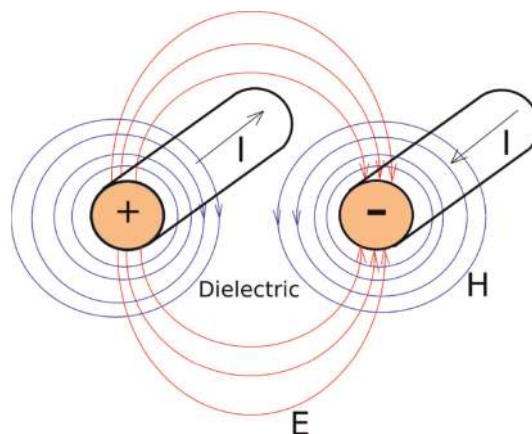


**Figure 3.**  
Section of the two-wire transmission line with the electric and magnetic fields.

transmission lines are used to measure the electrical properties of a dielectric material located inside the coaxial transmission line, as shown in **Figure 4**.

By analyzing the circuit model of a transmission line, the currents and voltages that propagate along it can be determined, using the circuit theory [22]. The equivalent circuit model of a transmission line can be seen in **Figure 5**. According to the equivalent circuit model of a transmission line, the characteristic impedance  $Z_0$  and the propagation constant  $\gamma$  can be expressed thus [21]:

$$Z_0 = \sqrt{\frac{R + j\omega L}{G + j\omega C}} \quad (13)$$

$$\gamma = \sqrt{(R + j\omega L)(G + j\omega C)} \quad (14)$$

where  $R$  is the series resistance per unit length [ $\Omega/m$ ];  $L$  is the series inductance per unit length [ $H/m$ ];  $C$  is the parallel capacity per unit length [ $F/m$ ];  $G$  is the parallel conductance per unit length [ $S/m$ ].

If the transmission line has no losses, it means that  $R = 0$  and  $G = 0$ ; then the characteristic impedance can be reduced as follows:

$$Z_0 = \sqrt{\frac{L}{C}} \quad (15)$$

$$\gamma = j\omega\sqrt{LC} \quad (16)$$

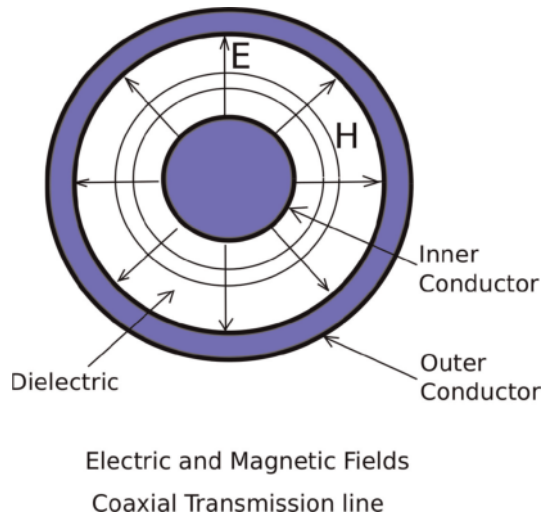


**Figure 4.** Section of coaxial transmission lines and the electric and magnetic fields.

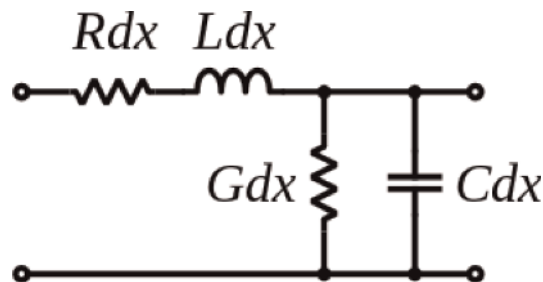


**Figure 5.** Distributed parameters of the transmission line.

The input impedance of a transmission line, with a material inside considering the material with dielectric losses, can be expressed thus [23]:

$$Z_i = Z_0 \frac{Z_L + Z_0 \tanh(\gamma l)}{Z_0 + Z_L \tanh(\gamma l)} \quad (17)$$

where  $\gamma$  is the propagation constant [ $1/m$ ];  $Z_L$  is the load impedance [ $\Omega$ ];  $l$  is the length of the transmission line from the load [ $m$ ];  $Z_0$  is the characteristic impedance of the transmission line [ $\Omega$ ].

#### 4. Time-domain measurement method of dielectric permittivity and conductivity of soils (TDR)

The time-domain reflectometry (TDR) is a well-known technique used to find the interruption point of the transmission lines in a CATV installation and is also useful to determine the dielectric permittivity (see **Figure 6**).

The time-domain reflectometry uses a step generator and an oscilloscope; a fast edge is launched into the transmission line under investigation, where the incident and reflected voltage waves on the transmission line are monitored by the oscilloscope. This method shows the losses and the characteristic impedance of the line: resistive, inductive, or capacitive [25]. The TDR method is based on the velocity of the electromagnetic wave that propagates through the soil, and the velocity of the wave depends on the water content of the soil. If a pulse is applied to a no-loss transmission line, the time domain graphic can be shown like in **Figure 7**. Considering the soil like a nonmagnetic media with low dielectric loss is [26, 27]:

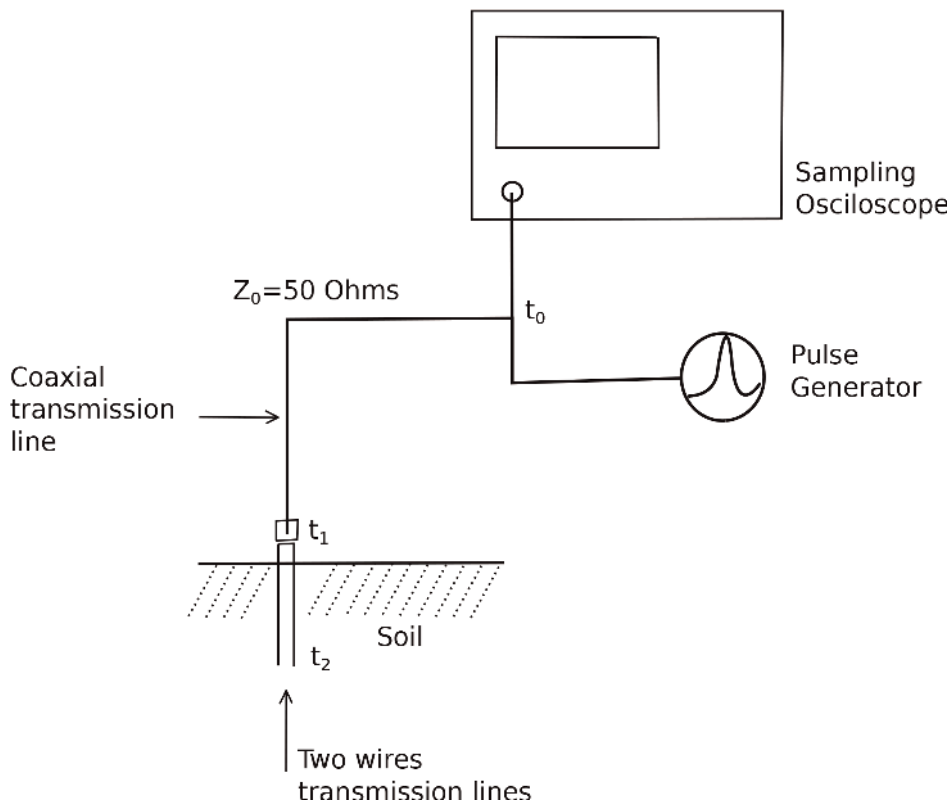


**Figure 6.** Setup of the dielectric measurement by the TDR method [24].

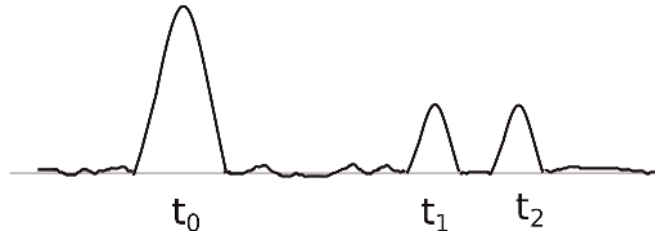


**Figure 7.**  
Propagation of the pulses in the time domain graphic with dielectric air [24].

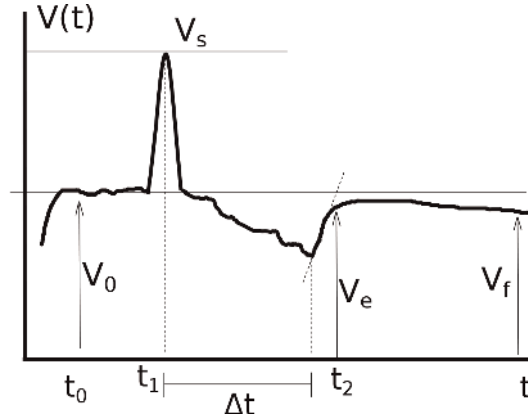


**Figure 8.**  
Picture of the voltage as a function of time for the probe is in the soil [26].

$$v = \frac{c}{\sqrt{\epsilon}} \quad (18)$$

where  $c[m/s]$  is the light velocity;  $\epsilon$  is the electric permittivity of the soil under test.

The time interval  $\Delta t$  between the received pulse and incident pulse can be observed in **Figure 8**, and the velocity can be expressed thus:

$$v = \frac{c}{\sqrt{\epsilon}} = \frac{2L}{\Delta t} \quad (19)$$

where  $L$  is the probe length.  
Then

$$\epsilon = \left( \frac{c\Delta t}{2L} \right)^2 \quad (20)$$

Usually the transmission line probes have a minimum length of 15 cm, because the incident electromagnetic wave takes a time of 1 ns in air in order to return to the input of the line. This time is too short to be measured.

The conductivity of the soil can be determined computing the reflected pulses in the probe in the time domain graphic (see **Figure 8**) [26, 28]. Numerous methods have been proposed by researchers; one of these is the procedure of Dalton et al. (1984) [26]:

$$\sigma_{dalton} = \left( \frac{\sqrt{\epsilon}}{120\pi L} \ln \left( \frac{V_f}{V_e - V_f} \right) \right) \quad (21)$$



where  $V_0$  is the amplitude of the TDR pulse;  $V_s$  is the amplitude after reflection from the start of the probe;  $V_e$  is the amplitude after reflection from the end of the probe;  $V_f$  is the reflected signal after a very long time.

Also the conductivity can be expressed thus [29]:

$$\sigma = \frac{K}{Z_0} \left( \frac{1 - \rho}{1 + \rho} \right) \quad (22)$$

where:

$$\rho = \frac{V_f - V_0}{V_0}$$

$Z_0$  is the characteristic impedance of the transmission line.

$K$  is a geometric constant of the probe, and it is experimentally determined by immersing the probe in solutions of known electrical conductivity  $Nt$  at temperature:

$$K = EC \cdot RL \cdot ft^{-1} (m)^{-1}$$

Temperature correction  $fT = 1 + KT(T - 25)$   $KT$  depends on the used solution.  $KT = 0.0191$  for a 0.01 M KCl solution.

## 5. Measurement method of dielectric permittivity and conductivity of soils in frequency domain

This method is based on the measurement of the reflection coefficient by means of the vector network analyzer (VNA) on the frequency domain of a coaxial transmission line in the soil; this can be observed in **Figure 9** [30–32].

The vector network analyzer can measure the scattering coefficient of a two-port passive network where the reflection coefficient in voltage  $\Gamma$  is  $S_{11}$  [34]. The probe impedance with the material inside is related with the reflected coefficient  $\Gamma$  [31]:

$$\frac{Z_p}{Z_0} = \frac{1 + \Gamma}{1 - \Gamma} \quad (23)$$

where  $Z_p$  is the impedance of the probe at the load and  $Z_0$  is the characteristic impedance of the probe.

The impedance of the probe can be calculated thus:

$$Z_p = \frac{2 \log \frac{B}{A}}{\sqrt{c\epsilon^*}} \cotangh \frac{\omega L \sqrt{\epsilon^*}}{c} j \quad (24)$$

where  $L$  is the electric length of the probe;  $c$  is the speed of light;  $L$  is the coaxial probe of length;  $A$  is the inner diameter;  $B$  is the outer diameter.

Then the complex electric permittivity for frequencies lower than 50 MHz can be approximated thus [31]:

$$\epsilon = \left( \frac{\frac{L}{2 \log \frac{B}{A}}}{\frac{1}{Z_T \omega j} - C_s} + \frac{\omega^2 L^2}{3c^2} \right)^{-1} \quad (25)$$

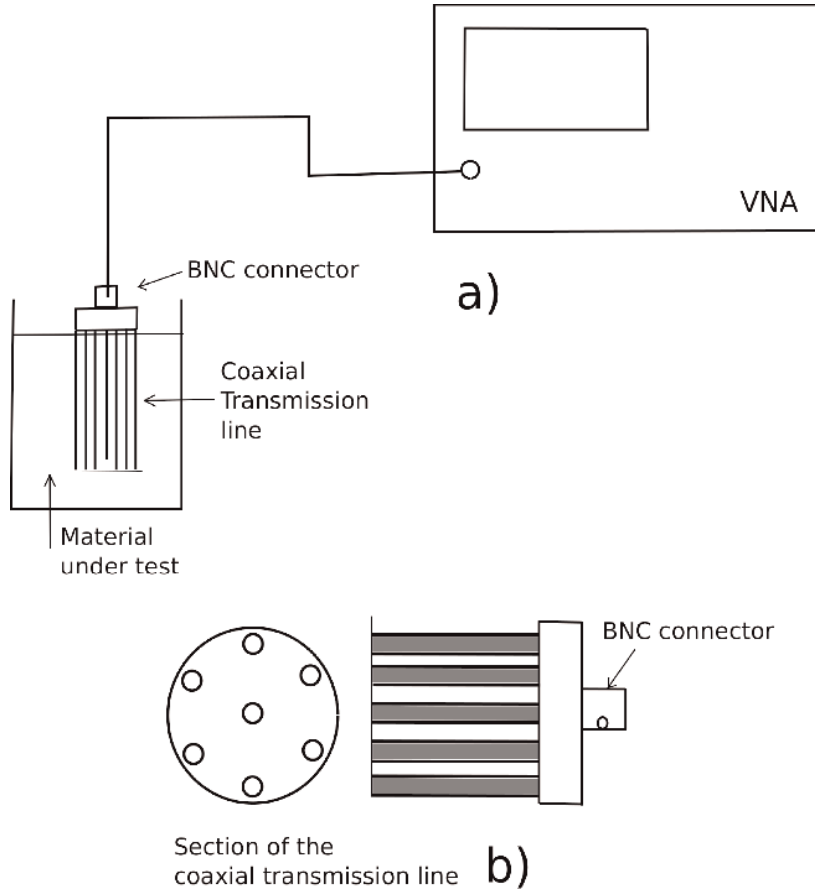


**Figure 9.** Dielectric measurement by the coaxial transmission line method. (a) Setup of the measurement experiment; (b) section of the transmission line and the material under test [33].

## 6. Dielectric measurement by the characteristic impedance of a transmission line in frequency domain

Some references of these measurement methods by means of characteristic impedance have been developed [35, 36]. This method is shown in **Figure 10**.

The input impedance can be computed by Eq. (17) for two different loads' impedance:

(a) Open circuit in the load  $Z_L \rightarrow \infty$

$$Z_i|_{Z_L=\infty} = \frac{Z_0}{\tanh(\gamma l)} = Z_0 \tanh^{-1}(\gamma l) \quad (26)$$

(b) Short circuit in the load  $Z_L = 0$

$$Z_i|_{Z_L=0} = Z_0 \tanh(\gamma l) \quad (27)$$

where, in general, the material inside the transmission line could be a dielectric loss; the propagation constant can be written thus:

$$\gamma = \alpha + j\beta \quad (28)$$

where  $\alpha$  is the attenuation constant [Neper/m] and  $\beta$  is the phase constant [rad/m].

Using Eqs. (26) and (27)

$$\gamma|_{Z_L \rightarrow \infty} = \frac{1}{l} \operatorname{atanh} \left( \frac{Z_0}{Z_i} \right) \quad (29)$$

$$\gamma|_{Z_L=0} = \frac{1}{l} \operatorname{atanh} \left( \frac{Z_i}{Z_0} \right) \quad (30)$$

Using the relation between  $\ln(x)$  and  $\operatorname{th}^{-1}(x)$

$$\gamma|_{Z_L \rightarrow \infty} = \frac{1}{2l} \ln \frac{Z_0 + Z_i}{Z_0 - Z_i} \quad (31)$$

$$\gamma|_{Z_L=0} = \frac{1}{2l} \ln \frac{Z_i + Z_0}{Z_i - Z_0} \quad (32)$$

The argument of the  $\ln$

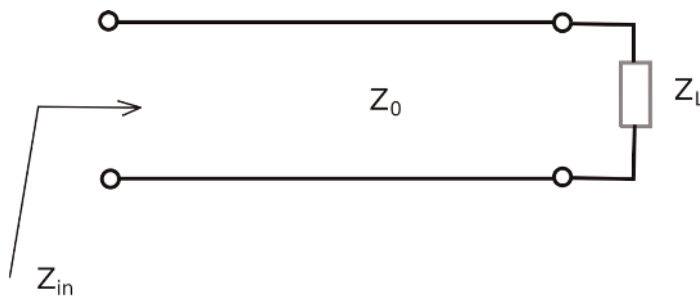
$$\gamma|_{Z_L \rightarrow \infty} = \frac{1}{2l} \ln (\rho_1 e^{j\phi_1}) \quad (33)$$

$$\gamma|_{Z_L=0} = \frac{1}{2l} \ln (\rho_2 e^{j\phi_2}) \quad (34)$$

Replacing the  $\ln$

$$\gamma|_{Z_L \rightarrow \infty} = \frac{1}{2l} \ln (\rho_1 e^{j\phi_1}) = \frac{1}{2l} [\ln (\rho_1) + \ln (e^{j\phi_1}) + j2k\pi] \quad k = 0, 1, 2, 3, \dots \quad (35)$$

$$\gamma|_{Z_L=0} = \frac{1}{2l} \ln (\rho_2 e^{j\phi_2}) = \frac{1}{2l} [\ln (\rho_2) + \ln (e^{j\phi_2}) + j2k\pi] \quad k = 0, 1, 2, 3, \dots \quad (36)$$



$Z_{in}$ : Input Impedance of the transmission line

$Z_L$ : Load impedance

$Z_0$ : Characteristic impedance

**Figure 10.**  
 Input impedance of the transmission line for  $Z_L = 0$  and  $Z_L \rightarrow \infty$ .

Then the propagation constant can be written thus:

$$\begin{aligned}
 \alpha|_{Z_L \rightarrow \infty} &= \frac{1}{2l} \ln(\rho_1) \\
 \beta|_{Z_L \rightarrow \infty} &= \frac{1}{2l} [\phi_1 + 2k\pi] \quad k = 0, 1, 2, 3, \dots \\
 \alpha|_{Z_L=0} &= \frac{1}{2l} \ln(\rho_2) \\
 \beta|_{Z_L=0} &= \frac{1}{2l} [\phi_2 + 2k\pi] \quad k = 0, 1, 2, 3, \dots
 \end{aligned} \tag{37}$$

By these last equations, the attenuation constant and the phase constant can be calculated with  $Z_i|_{Z_L=0}$  or  $Z_L \rightarrow \infty$ .

### 6.1 Determining $\epsilon$ and $\sigma$ from the propagation constant

The propagation constant  $\gamma$  can be written thus [11]:

$$\gamma = \sqrt{j\omega\mu(\sigma + j\omega\epsilon)} \tag{38}$$

From Eqs. (38) and (28)

$$\gamma^2 = j\omega\mu(\sigma + j\omega\epsilon') = -\omega^2\mu\epsilon' + j\omega\mu\sigma \tag{39}$$

$$\gamma^2 = \alpha^2 - \beta^2 + 2j\alpha\beta = (\alpha^2 + \beta^2)e^{j2\text{atan}\left(\frac{\beta}{\alpha}\right)} \tag{40}$$

Equating real and imaginary parts of  $\gamma^2$  of Eqs. (39) and (40)

$$-\omega^2\mu\epsilon' = (\alpha^2 + \beta^2) \cos\left(2\text{atan}\left(\frac{\beta}{\alpha}\right)\right) \tag{41}$$

$$\omega\mu\sigma = (\alpha^2 + \beta^2) \sin\left(2\text{atan}\left(\frac{\beta}{\alpha}\right)\right)$$

$\epsilon$  and  $\sigma$  can be obtained:

$$\begin{aligned}
 \epsilon' &= \frac{(\alpha^2 + \beta^2) \cos\left(2\text{atan}\left(\frac{\beta}{\alpha}\right)\right)}{-\omega^2\mu} \\
 \sigma &= \frac{(\alpha^2 + \beta^2) \sin\left(2\text{atan}\left(\frac{\beta}{\alpha}\right)\right)}{\omega\mu}
 \end{aligned} \tag{42}$$

Another expression of  $\epsilon$  and  $\sigma$  is using Eqs.(39) and (40):

$$\begin{aligned}
 \gamma^2 &= j\omega\mu(\sigma + j\omega\epsilon') \\
 \gamma^2 &= \alpha^2 - \beta^2 + 2j\alpha\beta
 \end{aligned} \tag{43}$$

Equating real and imaginary part of Eq. (43)

$$\begin{aligned}
 \omega\mu\sigma &= 2\alpha\beta \\
 -\omega^2\mu\epsilon &= \alpha^2 - \beta^2
 \end{aligned} \tag{44}$$

## Results

$$\begin{aligned}\sigma &= \frac{2\alpha\beta}{\omega\mu} \\ \epsilon &= \frac{\beta^2 - \alpha^2}{\omega^2\mu}\end{aligned}\quad (45)$$

The series resistance of the conductor of the coaxial transmission line used is  $R_{in} \cong 10^{-3}\Omega/m$  ( $f = 100\text{MHz}$ )  $Z_L = 0$ . This resistance can be neglected, because it has no effect in the measured attenuation constant  $\alpha$ .

### 6.2 Measurement procedure of the $\epsilon$ and $\sigma$

1. The input impedances are measured for a load impedance at short circuit  $Z_L = 0$  and open circuit  $Z_L \rightarrow \infty$  (see Eqs. (26) and (27)).
2. The attenuation constant  $\alpha$  and phase  $\beta$  are calculated with the equations found ad hoc (see Eq. (37)).
3. The electric permittivity  $\epsilon$  and the electrical conductivity  $\sigma$  are calculated using the equations found in Section 6.1.

In this way, a practical method of measurement is available to determine the parameters of dielectric materials, using coaxial transmission lines, in the frequency range from 1 to 1000 MHz. A problem that appears when measuring dielectric materials is the connector that establishes the link between the coaxial transmission line and the vector impedance meter. A systematic error in the impedance measured is introduced.

Therefore, the study and correction of the mentioned error in the section will be carried out.

### 6.3 Transmission lines used

Three coaxial transmission lines of General Radio (GR) Type 874, with air dielectric, have been used with a length of 100, 200, and 300 mm. The main characteristics of the General Radio coaxial transmission lines, type 874, are the following:

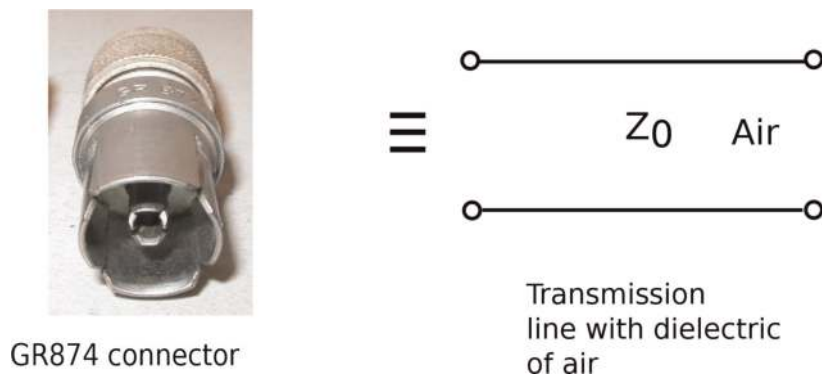


**Figure 11.**  
*N connector and its equivalent of a transmission line with dielectric of air.*

Characteristic impedance  $Z_0 = 50\Omega$ .  
 Input and output connector GR874

$$\begin{aligned} r_1 &= 12 \cdot 10^{-3}[m] \\ r_2 &= 5.2 \cdot 10^{-3}[m] \\ \sigma &\cong 5.810^7[S/m] \end{aligned}$$

#### 6.4 Correction error produced by the connector of the transmission line

It is important to perform the correction of the impedance introduced by the connector of the transmission line used. This connector is shown in **Figure 11**, and it is composed by a dielectric of very low dielectric losses and has a length of 10 mm (**Figure 12**). The characteristic impedance of the connector is practically  $Z_0 = 50\Omega$  with no losses [36]:

$$\gamma = \alpha + j\beta \cong j\beta \quad (46)$$

The input impedance to the connector can be written thus:

$$Z_i = Z_{0con} \frac{Z_L + jZ_{0con}tg(\beta x)}{Z_{0con} + jZ_Ltg(\beta x)} \quad (47)$$

where  $x$  is the length of the transmission line [m].

The electric permittivity of the dielectric of the connector is unknown; then it is easy to assume a transmission line with air equivalent to the connector with  $\epsilon = \epsilon_0$ ,  $\mu = \mu_0$ , and  $Z_{0con} = 50\Omega$ .

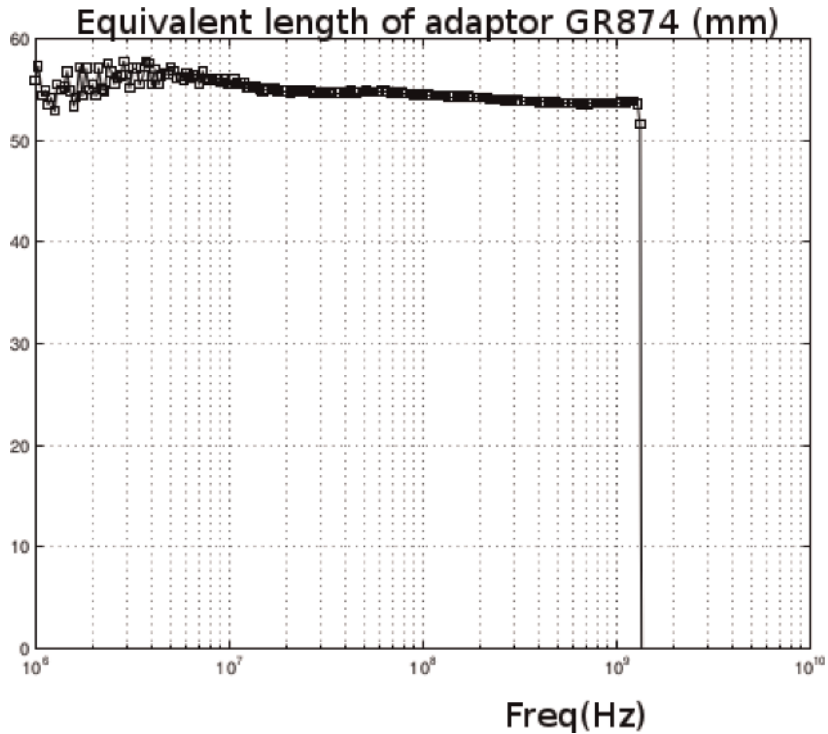


**Figure 12.**  
 Equivalent length of the transmission line of the connector GR874.

Considering the connector with no losses

$$\begin{aligned} \alpha &= 0 \\ \beta &= \omega_0 \sqrt{\mu_0 \epsilon_0} \end{aligned} \quad (48)$$

Then the input impedance of the connector with  $Z_L = 0$  is

$$Z_i|_{Z_L=0} = jZ_{0con} \operatorname{tg}(\beta x) \quad (49)$$

where  $x$  is the length of the connector of the equivalent transmission line. The length  $x$  of this equivalent transmission line can be written thus:

$$x = \frac{1}{\beta} \operatorname{tg}^{-1} \left( \frac{Z_{icon}|_{Z_L=0}}{jZ_{0con}} \right) \quad (50)$$

## 6.5 Results and discussion

### 6.5.1 Method of measurement

The experimental results of the electric conductivity and the dielectric permittivity measurement of the dry sand can be observed in **Figures 13** and **14**. In **Figure 13**, the electric conductivity as a function of the frequency, by means of the capacitive method, and the three types of transmission line lengths have been measured:  $L = 100, 200,$  and  $300$  mm; the convergence of all measurements are evident.

In **Figure 14**, the relative electric permittivity as a function of the frequency, by means of the capacitive method, and the three types of transmission line lengths

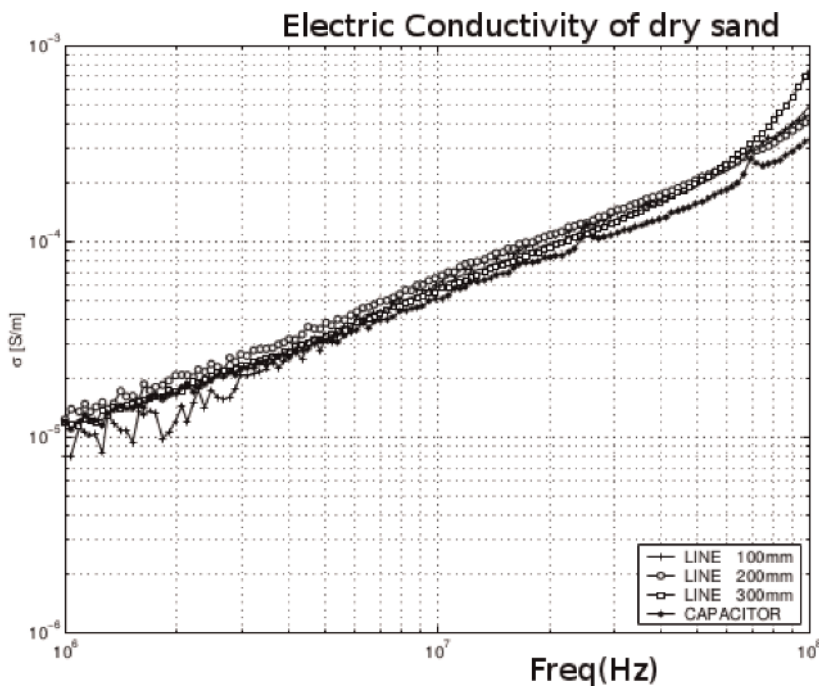


**Figure 13.** Electric conductivity as a function of the frequency for dry sand samples, using a capacitive method and three transmission lines: 100, 200, and 300 mm.

have been measured:  $L = 100, 200,$  and  $300$  mm; there is a convergence of all measurements. It is important to note that the shorter transmission line has a wider bandwidth of measurement. The transmission line length of  $L = 300\text{mm}$  shows the useful results up to  $30$  MHz; with a TL length of  $L = 200\text{mm}$ , the useful results are up to  $50$  MHz; and with a TL length of  $L = 100\text{mm}$ , the useful results are up to  $300$  MHz.

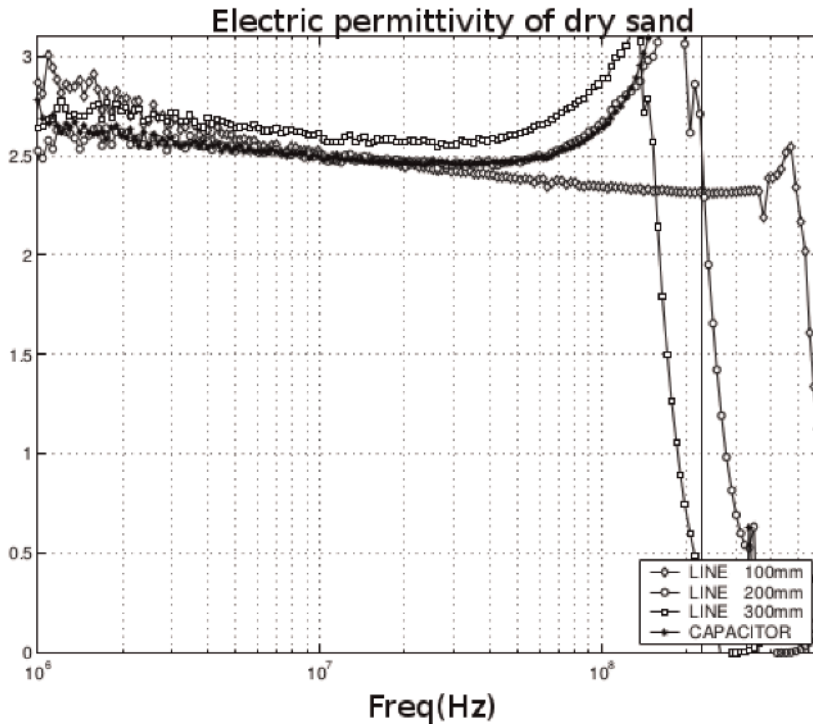


**Figure 14.** The relative dielectric permittivity as a function of the frequency for dry sand samples has been measured, using a capacitive method and three transmission lines: 100, 200, and 300 mm.

freq. (MHz)	Capacitor	T. line 100 mm	T. line 200 mm	T. line 300 mm	Expected value	Std. dev
1	2.80	2.86	2.65	2.65	2.74	0.034
2	2.60	2.76	2.62	2.75	2.68	0.021
3	2.60	2.70	2.60	2.70	2.65	0.010
5	2.50	2.61	2.57	2.65	2.58	0.012
7	2.50	2.54	2.55	2.62	2.55	0.0075
10	2.50	2.51	2.50	2.60	2.52	0.0073
20	2.40	2.45	2.47	2.57	2.47	0.0153
30	2.40	2.42	2.46	2.57	2.46	0.0173
50	2.40	2.40	2.46	—	2.41	0.0028
70	—	2.37	—	—	—	—
100	—	2.35	—	—	—	—

**Table 1.** Relative electric permittivity of dry sand.



freq. (MHz)	Capacitor	T. line 100 mm	T. line 200 mm	T. line 300 mm	Expected value	Std. dev
1	1	1.1	1.3	1.2	1.15	0.13
2	1.6	2.0	1.7	1.7	1.75	0.17
3	2.1	2.6	2.3	2.2	2.30	0.22
5	3.2	3.1	3.3	3.1	3.20	0.096
7	4.4	5	4.3	4	4.40	0.42
10	6.0	6.5	5.5	5.1	5.80	0.6
20	10	11	9.4	8.4	9.70	1.08
30	14.4	14.6	12.7	11.1	13.20	1.60
50	21.9	21.5	20.8	16	20.00	2.7

**Table 2.**  
 Electric conductivity of dry sand  $\sigma$  [ $\frac{S}{m} \cdot 10^{-5}$ ].

The expected value of the dielectric permittivity measured for the dry sand by means of a parallel plate capacitor and the three transmission lines used are shown in **Table 1**. The standard deviation of the three measurements shows a good agreement up to the vicinity of the resonant frequency of each transmission line. In **Table 2**, the electric conductivity of the dry sand can be observed. These curves have the same slope and show a good convergence.

### 6.5.2 Applications

The values of the electrical conductivity and the electrical permittivity are very useful to evaluate the propagation of surface waves in real ground, where the attenuation depends mostly on the conductivity of the soil. Such is the case that AM transmitters include radials, which consist of metallic conductors, placed at the base of the monopole antenna to increase conductivity, and in this way the losses due to Joule effect on the earth's surface are reduced. When the conductivity of the soil is perfect, the electric field vector that propagates will be perpendicular to the earth's surface; however, in real soils the electric field vector tilts and partly spreads into the earth, which dissipates power and transforms into heat [2]. This constitutes losses on earth.

Apparent soil electrical conductivity (ECa) to agriculture has its origin in the measurement of soil salinity, in arid-zone problem, which is associated with irrigated agricultural land. ECa is a quick, reliable, easy-to-take soil measurement that often relates to crop yield. For these reasons, the measurement of ECa is among the most frequently used tools in precision agriculture research for the spatiotemporal characterization of edaphic and anthropogenic properties that influence crop yield [37]. There are portable instruments for measuring the electrical conductivity of the soil by the method of electromagnetic induction and by the method of the four conductors, which are installed in the agricultural machinery to obtain a map of the soil, before carrying out the work of tilling the earth.

For geophysics applications, the solar disturbances (flares, coronal mass ejections) create variations of the Earth's magnetic field. These geomagnetic variations induce a geoelectric field at the Earth's surface and interior. The geoelectric field in turn drives geomagnetically induced currents, also called telluric currents along electrically conductive technological networks, such as power transmission lines, railways, and pipelines [38]. This geomagnetically induced currents create conditions where enhanced corrosion may occur. Earth conductivity can create

geomagnetically induced current variations, in particular where a pipeline crosses a highly resistive intrusive rock. It is important to make pipeline surveys once a year to measure the voltage at test posts to ensure that pipe-to-soil potential variations are within the safe range, impressed by cathodic protection systems [38].

## **Author details**

Walter G. Fano  
Faculty of Engineering, Universidad de Buenos Aires, Buenos Aires, Argentina

\*Address all correspondence to: [gustavo.gf2005@gmail.com](mailto:gustavo.gf2005@gmail.com)

## **IntechOpen**

---

© 2019 The Author(s). Licensee IntechOpen. This chapter is distributed under the terms of the Creative Commons Attribution License (<http://creativecommons.org/licenses/by/3.0>), which permits unrestricted use, distribution, and reproduction in any medium, provided the original work is properly cited. 

## References

- [1] Joffe E, Kai-Sang L. *Grounds for Grounding: A Circuit to System Handbook*. Piscataway, NJ, USA: Wiley, IEEE Press; 2009
- [2] Trainotti V, Fano WG, Dorado L. *Ingenieria Electromagnetica, Vol. 2*. 1st ed. Buenos Aires, Argentina: Nueva Libreria; 2006
- [3] Norton KA. The physical reality of space and surface waves in the radiation field of radio antennas. *Proceedings of the Institute of Radio Engineers*. 1937; **25**:1192-1202
- [4] Angulo I, Barclay L, Chernov Y, Deminco N, Fernandez I, Gil U, et al. *Handbook on Ground Wave Propagation*. Geneva, Switzerland: Radiocommunication Bureau, ITU; 2014
- [5] Corwin DL, Lesch SM. Application of soil electrical conductivity to precision agriculture. *American Society of Agronomy*. 2003; **95**(3):455-471
- [6] Smith-Rose RL. The electrical properties of soil for alternating currents at radio frequencies. *Proceedings of the Royal Society of London*. 1933; **140**:359-377
- [7] Jol HM. *Ground Penetrating Radar Theory and Applications*. Oxford, UK: Elsevier Science; 2009
- [8] Ramo S, Whinnery J, Van Duzer T. *Fields and Waves in Communication Electronics*. India: Wiley; 2008
- [9] Griffiths DJ. *Introduction to Electrodynamics*. 4th ed. Boston, MA: Pearson; 2013. Re-published by Cambridge University Press in 2017
- [10] Reitz JR, Milford FJ, Christy RW. *Foundations of Electromagnetic Theory*. 4th ed. USA: Addison-Wesley Publishing Company; 2008
- [11] Trainotti V, Fano WG. *Ingenieria Electromagnetica, Vol. 1*. 1st ed. Buenos Aires, Argentina: Nueva Libreria; 2004
- [12] Stratton JA. *Electromagnetic Theory*. Hoboken, New Jersey, USA: IEEE Press, Wiley-Interscience; 2007
- [13] Samoulian A, Cousin I, Tabbagh A, Bruand A, Richard G. Electrical resistivity survey in soil science: A review. *Soil and Tillage Research*. 2005; **83**(2):173-193
- [14] Abu-Hassanein ZS, Benson CH, Blotz LR. Electrical resistivity of compacted clays. *Journal of Geotechnical Engineering*. 1996; **122**(5): 397-406
- [15] Hoekstra P, Delaney A. Dielectric properties of soils at uhf and microwave frequencies. *Journal of Geophysical Research*. 1974; **79**:11, 1699-1708
- [16] Peplinski NR, Ulaby FT, Dobson MC. Dielectric properties of soils in the 0.3–1.3-GHz range. *IEEE Transactions on Geoscience and Remote Sensing*. 1995; **33**:803-807
- [17] El-rayes MA, Ulaby FT. Microwave dielectric spectrum of vegetation—Part I: Experimental observations. *IEEE Transactions on Geoscience and Remote Sensing*. 1987; **GE-25**:541-549
- [18] Ulaby FT, El-rayes MA. Microwave dielectric spectrum of vegetation—Part II: Dual-dispersion model. *IEEE Transactions on Geoscience and Remote Sensing*. 1987; **GE-25**:550-557
- [19] Hipp JE. Frequency dispersion of complex permeability in mnzn and nzn

- spinel ferrites and their composite materials. Proceedings of the IEEE. 1974;**62**:98-103
- [20] Fano WG, Trainotti V. Dielectric properties of soils. In: 2001 Annual Report Conference on Electrical Insulation and Dielectric Phenomena (Cat. No.01CH37225); 2001. pp. 75-78
- [21] Karakash J. Transmission Lines and Filter Networks. New York, USA: Macmillan; 1950
- [22] Peterson A, Durgin DG. Transient signals on transmission lines: An introduction to non-ideal effects and signal integrity issues in electrical systems. Synthesis Lectures on Computational Electromagnetics. 2008;**3**(1):1-144
- [23] Collin R. Foundations for Microwave Engineering. 2nd ed. New York, USA: Wiley India Pvt. Limited; 2007
- [24] Olchawa O, Kumor M. Time domain reflectometry (TDR) measuring dielectric constant of polluted soil to estimate diesel oil content. Archives of Hydro-Engineering and Environmental Mechanics. 2008;**55**(1-2):55-62
- [25] Keysight. Time domain reflectometry theory. Keysight Technologies; Application Note; 2015
- [26] Zante P. Water content and soil bulk electrical conductivity measurements. TDR Technology Applied to Soils. 2002;**49**(1):1-27
- [27] Robinson DA, Jones SB, Wraith JM, Friedman SP. A review of advances in dielectric and electrical conductivity measurement in soils using time domain reflectometry. Vadose Zone Journal. Soil Science Society of America. 2003;**2**:444-475
- [28] Evett SR. Coaxial multiplexer for time domain reflectometry measurement of soil water content and bulk electrical conductivity. Transactions of the ASAE. 1998;**41**(2): 361
- [29] Ebrahimi-Birang N, Maul CP, Morley WA. Calibration of a TDR instrument for simultaneous measurements of soil water and soil electrical conductivity. Transactions of the ASABE (American Society of Agricultural and Biological Engineers). 2006;**49**(1):75-82
- [30] Seyfried MS, Murdock MD. Measurement of soil water content with a 50-MHz soil dielectric sensor. Soil Science Society of America Journal. 2004;**68**:394-403
- [31] Campbell JE. Dielectric Properties of Moist Soils at rf and Microwave Frequencies. New Hampshire, USA: Dartmouth Digital Library Collections; 1988
- [32] ZChaudhari HC, Shinde VJ. Dielectric properties of soils at x-band microwave frequency. Indian Journal of Pure and Applied Physics. 2012;**50**(1): 64-66
- [33] La Gioia A, Porter E, Merunka I, Shahzad A, Salahuddin S, OHalloran M. Open-ended coaxial probe technique for dielectric measurement of biological tissues: Challenges and common practices. Diagnostics. 2018;**8**(2):2-38
- [34] Pozar D. Microwave Engineering. 4th ed. Hoboken, NJ, USA: Wiley; 2011
- [35] Kirkscether EJ. Ground constant measurements using a section of balanced two-wire transmission line. IRE Transactions on Antennas and Propagation. 1960:307-312
- [36] Fano W. Interacción de la radiación electromagnética Con Materiales dieléctricos y magnéticos. Aplicaciones. PHD Thesis. Universidad de Buenos Aires, Buenos Aires, Argentina; 2004

[37] Corwin D, Lesch S. Apparent soil electrical conductivity measurements in agriculture. *Computers and Electronics in Agriculture*. 2005;**46**(1):11-43

[38] Fernberg PA, Samson C, Boteler DH, Trichtchenko L, Larocca P. Earth conductivity structures and their effects on geomagnetic induction in pipelines. *Annales Geophysicae*. 2007; **25**(1):207-218